Indian Journal of Chemistry
Vol. 62, July 2023, pp. 696-702
DOI: 10.56042/ijc.v62i7.999

Thiophene functionalized naphthalene diimide for the sensitive detection of nitroaromatics

Dnyaneshwar I Bhusanur[a,e], Prabhat K Singh[b,c], Sheshanath V Bhosale[d] & Sidhanath V Bhosale[a,e]*

[a] Polymers and Functional Materials Division, CSIR-Indian Institute of Chemical Technology, Hyderabad 500 007, Telangana, India

[b] Radiation and Photochemistry Division, Bhabha Atomic Research Centre, Mumbai 400 085, India

[c] Homi Bhabha National Institute, Training School Complex, Anushaktinagar, Mumbai 400 094, India

[d] Department of Chemistry, School of Chemical Sciences, Central University of Karnataka, Kadaganchi, Kalaburagi 585 367, Karnataka, India

[e] Academy of Scientific and Innovative Research (AcSIR), CSIR-HRDC Campus, Postal Staff College Area, Sector 19, Kamla Nehru Nagar, Ghaziabad 201 002, Uttar Pradesh, India

E-mail: bhosale@iict.res.in

Received 3 May 2023; accepted (revised) 13 June 2023

In recent years, the detection of nitroaromatics (NACs) has attracted the researchers' attention due to increased threats of terrorist and environmental protection. In this regard, *tetra*-thiophene (Th) functionalized naphthalene diimide (NDI) conjugate NDI-Th has been synthesized and confirmed *via* spectroscopic methods. UV-Vis and fluorescence methods have been utilized to examine the photophysical characteristics of NDI-Th in various solvent systems. Moreover, NDI-Th as a fluorescent sensor displays selective recognition of 2,4-dinitrophenol (DNP) and 2,4-trinitrophenol (TNP) with a limit of detection of 4.74×10^{-8} M and 7.60×10^{-8} M, respectively. Thus NDI-Th acts as a promising candidate for explosive multi-NACs detection.

Keywords: Thiophene, Naphthalene Diimide, Nitroaromatics, Sensor

In modern society, to counter terrorist activity, explosive detection is one of the most challenging tasks worldwide. Among the explosives, nitrogen-containing compounds, *i.e.*, nitroaromatics (NACs), have been utilized extensively as rocket fuels, in batteries, and in matches[1]. Such NACs create environmental pollution and health problems, *e.g.*, skin and eye irritation and damage to the respiratory system, kidney, and liver[2,3]. Therefore, the detection of such NACs can aid in controlling environmental pollution and anti-terrorism efforts[4]. Researchers have developed several detection techniques for NACs, which in turn rely on instrumental methods, *i.e.*, gas chromatography coupled with mass spectroscopy (GC-MS)[5], ion-mobility spectroscopy (IMS)[6], surface-enhanced Raman spectroscopy (SERS)[7], thermal neutron analysis, cyclic voltammetry[8,9], energy dispersive X-ray diffraction (EDXRD)[10], mass spectrometry[11] and high pressure liquid chromatography (HPLC)[12]. However, instrumental techniques required sophisticated protocols with a high cost and exhibited limitations such as poor portability, time-consuming calibration, and effective way of on-site applications. To overcome these limitations, researchers developed colorimetric and fluorescent protocols for NACs detection[13]. Among these two techniques, the fluorescence method may yield the best sensitivity towards NACs due to the emission signal observed at low background[14]. Small Organic molecules and polymeric materials are utilized for NAC explosives sensing[15-17]. Most of the fluorescent methods are based on the fluorescence quenching mechanism upon the interaction of the receptor with NACs. The fluorescence materials exhibited some drawbacks, such as emission quenching, photodegradation, and photobleaching of the organic materials. To overcome these limitations, the design and development of organic fluorescence materials for selective and selective NACs trace detection is still a challenging task.

Herein, we demonstrate the photophysical and sensing characteristics of NDI-Th (naphthalene diimide-thiophene), an organic molecular architecture fabricated from naphthalene diimide (NDI) and thiophene (Th). These complementary subunits were selected for their molecular structures

and photophysical properties. NDIs are aromatic π-conjugated chromophores exhibiting n-type semiconducting properties[18]. The structural manipulation of NDI at imide- and core- position makes it an attractive scaffold for various applications ranging from materials, chemosensing, bioimaging, and biological applications[19]. Core-substituted NDIs are extensively employed in sensing applications due to their optical and photophysical properties and ease of derivatisation[20,21]. Thiophene-containing organic molecules exhibited great potential in materials science. Thiophene-bearing π-systems display high charge transport characteristics and are widely employed in organic light emitting diodes (OLEDs), organic photovoltaics (OPVs), and organic field-effect transistors (OFETs)[22]. Moreover, a literature search revealed that the incorporation of thiophene in the organic fluorophore such as pentacenequinone (Fig. 1a)[23] and tetraphenyl ethylene (TPE)[24] (Fig. 1b) had been examined as fluorescent receptor for NACs. Thiophene (Th) played a pivotal role in enhancing the NACs recognition ability. In the design of NDI-Th, we demonstrate the selection of fluorophore and the introduction of Th, which in turn leads to enhanced NAC recognition properties. The detection limit of NDI-Th towards TNP and DNP were estimated to be 4.74×10^{-8} M and 7.60×10^{-8} M, respectively.

The synthetic route for NDI-Th is displayed in Scheme 1. In the first step, 2,3,6,7-tetrabromo-NDI **2** was synthesized *via* a bromination reaction of 1,4,5,8-naphthalenetetracarboxylic dianhydride **1** in the presence of H_2SO_4 and DBH[25]. Compound **3** was synthesized by treating **2** with 2-ethylhexyl amine in acetic acid, followed by phosphorus tribromide[25]. 2-Tributylstannylthiophene was utilized in a Still cross-coupling reaction with **3** to afford thiophene functionalized NDI (NDI-Th) (Scheme 1, Fig. 1a)[26]. NDI-Th was well characterized by ^{1}H and ^{13}C NMR spectroscopy, FT-IR, MALDI-TOF, and HRMS spectrometry. In the HRMS spectrum of NDI-Th, a peak corresponding to $[NDI\text{-}Th+H]^+$ appeared at *m/z* 819.2413 (Fig. S5, ESI†).

Photophysical studies

The UV-Vis spectra of NDI-Th (1×10^{-5} M) in different solvents such as THF, DCM, MeOH, ACN, and MCH were recorded (Fig. 2c). In DCM, NDI-Th exhibited absorption peaks at 259 nm (ε = 86800 M^{-1} cm^{-2}), 284 nm (ε = 26000 M^{-1} cm^{-2}), 360 nm (ε = 18200 M^{-1} cm^{-2}), 379 nm (ε = 16700 M^{-1} cm^{-2}),

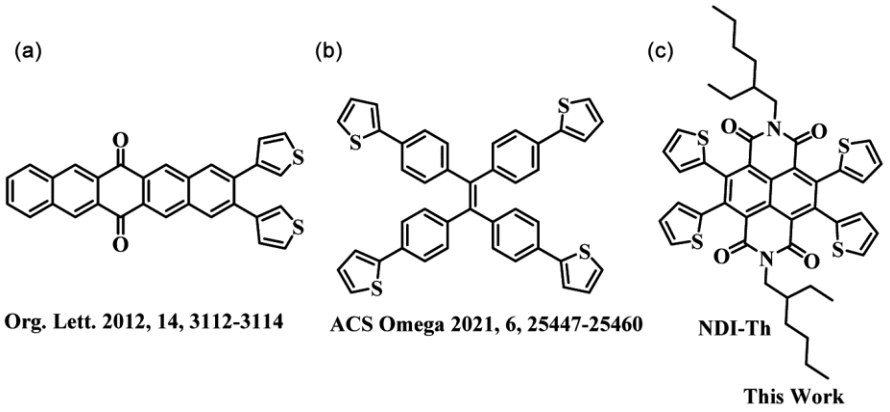

Fig. 1 — Molecular structures of the receptor for NACs sensing

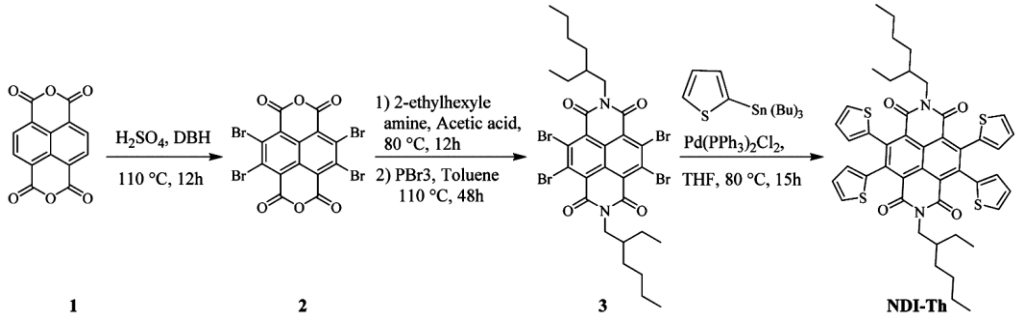

Scheme 1 — Synthetic route for NDI-Th

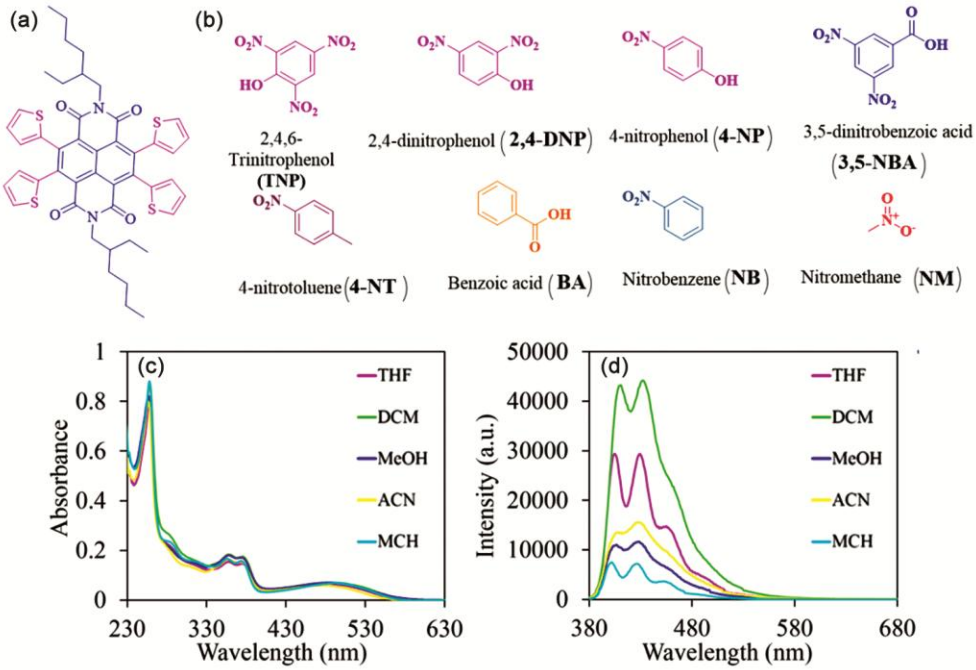

Fig. 2 — Molecular structure of (a) NDI-Th and (b) nitroaromatics, (c) UV-Vis spectra of NDI-Th (10 μM) and (d) Fluorescence spectra (λ_{ex} = 370 nm) of NDI-Th (10 μM) in different solvents at RT.

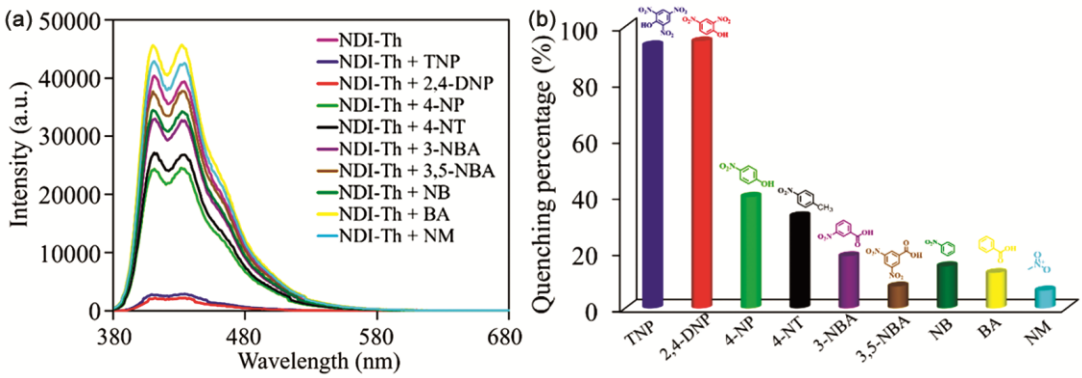

Fig. 3 — (a) Fluorescence spectra (λ_{ex} = 370 nm) of NDI-Th (1×10^{-5} M) in DCM upon addition of 180 eq. of NACs, (b) Quenching percentage of NDI-Th upon the addition of various NACs respectively at RT.

and broad peak at 500 nm (ε = 6800 M^{-1} cm^{-2}). There were negligible shifts in the UV-Vis peaks of NDI-Th in THF, MeOH, ACN, and MCH (Fig. 2c), indicating no change in the ground state energy distribution of NDI-Th. The fluorescence spectra of NDI-Th (1×10^{-5} M) in DCM, upon excitation at 370 nm, displayed two strong fluorescence emission peaks at 411 nm and 434 nm, and a shoulder peak at 466 nm (Fig. 2d). Notably, as we transitioned from THF to ACN to MeOH to MCH, we observed a gradual decrease in fluorescence peak intensity. These findings suggest that solvent polarity exerts a significant influence on the fluorescence properties of NDI-Th[27].

NDI-Th exhibits strong fluorescence properties in DCM. Therefore, NDI-Th was explored as a sensor for the detection of NACs in DCM. The fluorescence intensity of NDI-Th quenching with the addition of various NACs is displayed in Fig. 3a and Fig. 3b. All the examined NACs, *e.g.*, 4-NP, 3,5-NBA, 4-NT BA, NB, and NM (Fig. 2b), exhibited negligible fluorescence emission quenching except TNP and DNP (Fig. 3a and Fig. 3b). The results displayed that the fluorescence quenching of NDI-Th in the presence of NACs containing only one hydroxyl group followed the order of TNP (Fig. 3b, blue bar) ≥ DNP (Fig. 3b, red bar) > NP (Fig. 3b, green bar), with both

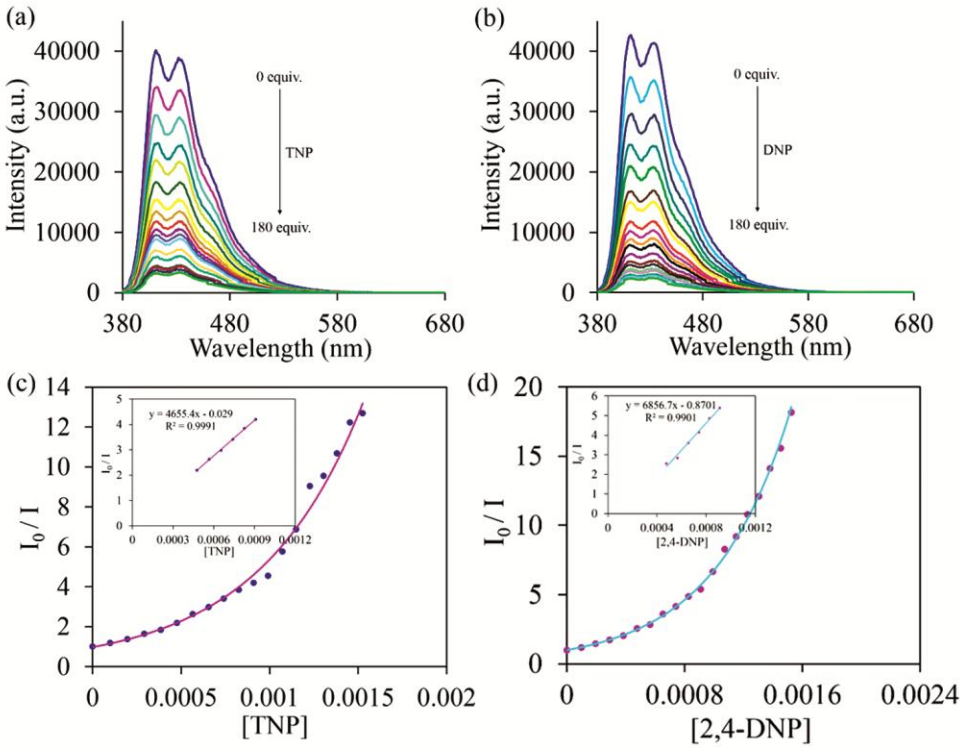

Fig. 4 — (a) FL spectra (λ_{ex} = 370 nm) of NDI-Th (1×10^{-5} M) in DCM upon addition of TNP (0 to 180 eq.) at RT, (b) FL spectra (λ_{ex} = 370 nm) of NDI-Th (1×10^{-5} M) in DCM upon addition of 2,4-DNP (0 to 180 eq.) at RT, (c) Stern−Volmer plot for the quenching of NDI-Th with increasing concentration of TNP. The inset shows the initial concentration region of Stern-Volmer plot, (d) Stern−Volmer plot for NDI-Th with the increasing concentration of 2,4-DNP and in initial region of Stern-Volmer plot is shown in the inset.

TNP and DNP demonstrating the highest quenching efficiency compared to NP. Therefore, NDI-Th showed good selectivity towards TNP and DNP compared to other NACs.

Fluorescence study of nitroaromatics detection

Furthermore, to get detailed insight into the sensing properties of NDI-Th towards TNP and DNP, we performed fluorescence (FL) titration experiments. Upon the incremental addition of TNP to the NDI-Th in DCM, we found the gradual quenching in the fluorescence emission peak intensity (Fig. 4a). Similarly, with the gradual addition of DNP, we observed a systematic decrease in fluorescence emission intensity of NDI-Th (Fig. 4b). The fluorescence quenching efficiency was estimated using Stern-Volmer (SV) plots and equation. The fluorescence quenching response of NDI-Th, *i.e*., SV plots upon addition of TNP and DNP, were displayed in Fig. 4c and Fig. 4d, respectively. Incremental addition of TNP to NDI-Th exhibited an upward curve in the SV plot (Fig. 4c). At lower concentrations, a linear quenching response was observed (Fig. 4c, insight), indicating static quenching, whereas, at higher concentrations of TNP, the deviation of SV curve from linearity suggested dynamic quenching due to the resonance energy transfer. The SV constant was calculated using equation[28].

$$I_0/I = 1 + K_{SV}[Q] \quad \ldots (1)$$

The fluorescence peak intensities, I_0 and I, correspond to the absence and presence of NACs, respectively. The concentration of the analyte being measured is represented by [Q], while K_{SV} stands for the Stern-Volmer constant.

The estimated SV constant for NDI-Th with the addition of TNP and DNP was found to be 4.65×10^3 M^{-1} and 6.85×10^3 M^{-1}, respectively.

To examine the NDI-Th practical application, the limit of detection (LOD) was estimated to determine the receptor's sensitivity. Fig. 5a and Fig. 5b show the calibration curves of NDI-Th with the decrease in fluorescence intensity with increasing concentrations of TNP and DNP, respectively. The initial region (inset) of the calibration curves from Fig. 5a and Fig. 5b were utilized to calculate the LOD of NDI-Th towards TNP and DNP, respectively.

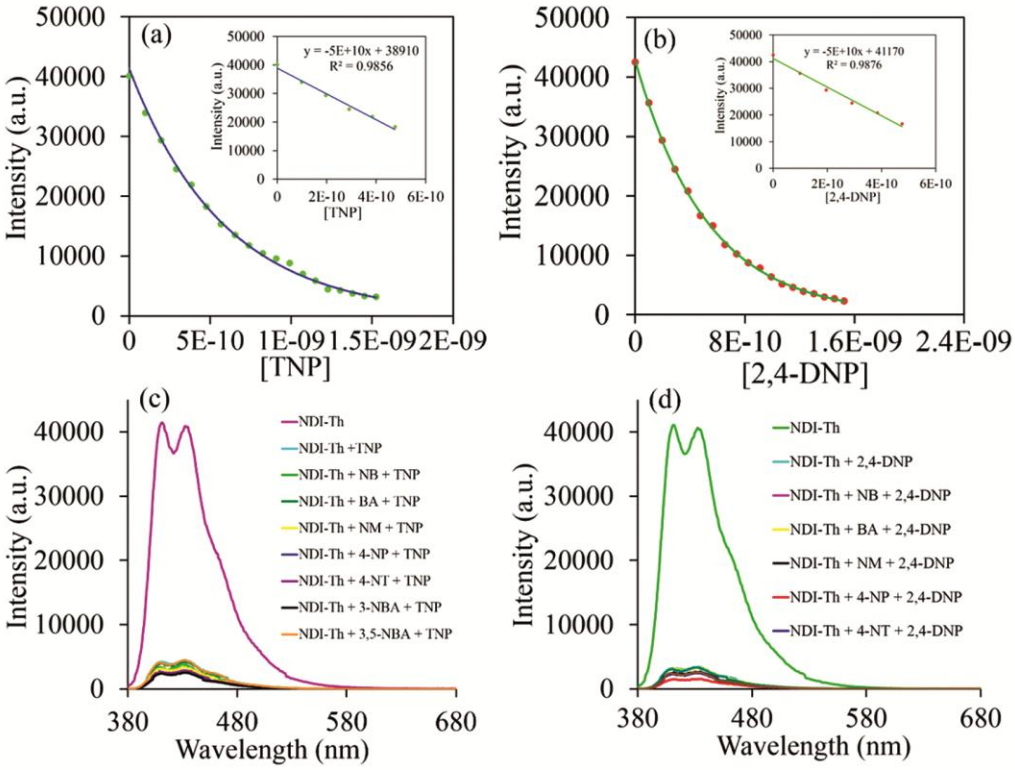

Fig. 5 — (a) Calibration curve of NDI-Th *vs* increasing concentration of TNP (0 to 180 eq) at 411 nm, (b) Calibration curve of NDI-Th *vs* increasing concentration of 2,4-DNP (0 to 180 eq) at 411 nm, (c) Fluorescence spectra of NDI-Th (1×10^{-5} M) in DCM with the addition of TNP in the presence of other NACs (180 eq) at RT, (d) Fluorescence spectra of NDI-Th (1×10^{-5} M) in DCM upon addition of 2,4-DNP in the presence of other NACs (180 eq) at RT.

$$LOD = 3\sigma/K \quad \ldots (2)$$

Where σ is the standard deviation

K is the slope from the intensity *versus* sample concentration plot.

From the slope of the curves, estimated LOD was found to be as low as 4.74×10^{-8} M and 7.60×10^{-8} M for TNP and DNP, respectively, which is comparable to the literature reported values.

Further, we examined the sensitivity of NDI-Th towards TNP and DNP in the presence of potentially competitive NACs (Fig. 5c, Fig. 5d, and Fig. S6a and S6b). As shown in Fig. 5c, the competitive experiments of NDI-Th displayed a remarkable fluorescence response towards TNP upon the addition of other NACs, indicating that NDI-Th could be a promising sensor for TNP. A similar trend was also observed for DNP addition to NDI-Th in the presence of other interfering NACs (Fig. 5d). Therefore, we could employ the NDI-Th receptor for the selective detection of TNP and DNP in actual samples.

Experimental Section

Materials and Methods

Chemicals and solvents were obtained from various sources including Sigma Aldrich, India, Alfa Aesar, India, TCI, India, and Finar, India, and were used as received. The FT-IR spectra were obtained using a Thermo Nicolet Nexus 670 FT-IR spectrometer, while ^{1}H and ^{13}C NMR spectra were measured using Bruker Avance 400 or 500 MHz and 100 MHz spectrometers, respectively. The ESI-MS spectra of the synthesized compounds were acquired using Shimadzu Lab solutions, and MALDI-TOF measurements were performed using a Shimadzu Biotech Axima performance spectroscopic instrument. Shimadzu UV-1800 spectrophotometer and RF-6000 were employed for absorbance and fluorescence measurements in solution form.

Synthesis of 2

In a 250 mL round-bottom flask, 2 g (7.45 mmol) of naphthalene-1,4,5,8-tetracarboxylic dianhydride (NDA) and 70 mL of sulphuric acid were added and

stirred at RT for 20 min. Then, 1,3-dibromo-5,5-dimethylhydantoin (DBH) was added in six portions over the course of 2 h and stirred for an extra 30 min at RT The reaction mixture was heated to 110°C and kept stirring for 16 h. The reaction progress was monitored using thin layer chromatography (TLC). After the completion of the reaction, the mixture was cooled and quenched with crushed ice before being filtered using a suction vacuum. The resulting residue was washed first with water followed by methanol. The obtained yellow solid of 2,3,6,7-tetrabromo-1,4,5,8-naphthalenetetracarboxylic dianhydride (3.2 g) was collected and dried in an oven. The 2,3,6,7-tetrabromo-NDI was used for the next step without any further purification.

4,5,9,10-Tetrabromo-2,7-bis(2-ethylhexyl)benzo [lmn][3,8]phenanthroline-1,3,6,8(2*H*,7*H*)-tetraone, 3

To a solution of compound **2** (2.5 g, 4.2 mmol) in 80 mL of acetic acid, 1.93 g (14.98 mmol) of 2-ethyl-1-hexylamine was added and stirred for 15 min at RT. The resulting mixture was then heated to 80°C and left to react for 12 h. Once the reaction was complete, the mixture was cooled to RT and poured into ice water. The yellow precipitate was collected by filtration and washed with water. The resulting crude product was then dried under vacuum and used directly in the next step.

The crude material obtained in the previous step (3.5 g, 4.15 mmol) was added to 70 mL of anhydrous toluene and stirred at RT for 10 min. PBr_3 (2.80 g, 10.38 mmol) was then added, and the mixture was refluxed at 110 °C for 48 h while monitoring the reaction progress by TLC. Once the reaction was complete, the mixture was allowed to cool to RT and then extracted with toluene (3×60 mL). The combined organic layer was dried over anhyd. Na_2SO_4, then concentrated under vacuum conditions. Subsequently, the crude product obtained was purified through column chromatography, employing a hexane: dichloromethane mixture as the eluent. This yielded **3** as a dark yellow solid with a yield of 65%. ^{1}H NMR (400 MHz, $CDCl_3$): δ 4.19-4.17 (d, 4H), 1.97 – 1.92 (m, 2H), 1.40 – 1.36 (m, 16H), 0.96 – 0.930 (t, 6H), 0.90-0.87 (t, 6H); ^{13}C NMR (100 MHz, $CDCl_3$): δ 160.32, 135.37, 126.46, 125.85, 46.35, 37.84, 30.65, 28.52, 23.98, 23.10, 14.09, 10.60; MALDI-TOF: *m/z* Calcd for $C_{30}H_{34}Br_4N_2O_4$: 801.92. Found: 802.82 $[M+H]^+$.

2,7-bis(2-Ethylhexyl)-4,5,9,10-tetra(thiophen-2-yl) benzo[lmn][3,8]phenanthroline-1,3,6,8(2*H*,7*H*)-tetraone, NDI-Th

To a solution of compound **3** (0.500 g, 0.62 mmol) in 50 mL of anhydrous THF, tributyl(thiophen-2-yl) stannane (1.38 g, 0.30 mmol) and palladium (II) bis(triphenylphosphine) dichloride ($PdCl_2(PPh_3)_2$) were added under a nitrogen atmosphere. The reaction mixture was then heated to 80°C and left to react for 15 h, while monitoring the reaction progress by TLC. Upon completion of the reaction, the mixture was allowed to cool down to RT before the solvent was evacuated using a vacuum. The resulting crude product was subsequently purified through column chromatography, utilizing a hexane-dichloromethane mixture as the eluent. This yielded **NDI-Th** as a red solid with a yield of 80%. FT-IR (KBr): 3479, 2926, 2854, 1673, 1434, 1369, 1283, 1194, 841, 698 cm^{-1}; ^{1}H NMR (400 MHz, $CDCl_3$): δ 7.39-26 (m, J = 5.01, 1.22 Hz, 4H), 6.97-6.95 (m, J = 3.5 Hz, 4H), 6.66-6.67 (m, J = 3.54, 1.10 Hz, 4H), 3.91-3.89 (t, 4H), 1.81-1.78 (m, 2H), 1.27-1.18 (m, 16H), 0.85-0.78 (t, 12H); ^{13}C NMR (100 MHz, $CDCl_3$): δ 161.81, 142.59, 138.73, 127.88, 127.08, 126.80, 125.79, 44.95, 37.25, 30.39, 28.55, 23.62, 23.17, 14.13, 10.51; MALDI-TOF: *m/z* Calcd for $C_{46}H_{46}N_2O_4S_4$: 818.23. Found: 819.28 $[M+H]^+$; HRMS: *m/z* Calcd for $C_{46}H_{47}N_2O_4S_4$: 819.2380. Found: 819.2413 $[M+H]^+$.

Conclusions

In summary, we developed thiophene-functionalized NDI as an explosive nitroaromatic sensor. NDI-Th showed efficient fluorescence quenching properties in the presence of TNP and DNP. The quenching constants for NDI-Th with the addition of TNP and DNP were 4.65×10^3 M^{-1} and 6.85×10^3 M^{-1}, respectively. Moreover, synthesized NDI-Th fluorophore can detect TNP and DNP with as low a detection limit of 4.74×10^{-8} M and 7.60×10^{-8} M, respectively. This work provides the significance of the thiophene subunit in improvement in NACs detection. Thus, the incorporation of thiophene in fluorophore moiety will become an increasingly important probe for the fluorescence detection of NACs.

Conflict of Interests

All authors declare there is no conflict of interest.

Supplementary Information

Supplementary information is available in the website http://nopr.niscpr.res.in/handle/123456789/58776.

Acknowledgments

SVB (IICT) is grateful for financial support from BRNS under the project No. 58/14/01/2020-BRNS/37047 and the Director, CSIR-IICT (MS No. IICT/Pubs./2023/126). DDB is grateful for financial support through SRF from CSIR, New Delhi. Sheshanath Vishwanath Bhosale (CUK) acknowledges University Grants Commission (UGC) Faculty Research Program, New Delhi, India (F.4-5(50-FRP) (IV-Cycle)/2017(BSR)) for an award of Professorship.

References

1 Keicher T, Mitchell A R, Pagoria P F & Schmidt R D, *Energetic Materials-Technology, Manufacturing and Processing, 27th Int Annual Conf FICT, Karlsruhe, Germany*, (The Institute) 1996 p. 29.
2 Hebert R M & Jackovitz A M, *Wildlife Toxicity Assessment for Picric Acid 2,4,6-Trinitrophenol*, (Elsevier Inc) 2015.
3 Yost S L, Pennington J C, Brannon J M & Hayes C A, *Mar Poll Bull*, 54 (2007) 1262.
4 Marshall M & Oxley J C, *Aspects of Explosives Detection*, 1st ed., (Elsevier, Amsterdam) 2009.
5 Walsh M E, *Talanta*, 54 (2001) 427.
6 Hakansson K, Coorey R V, Zubarev R, Talrose V L & Hakansson P, *J Mass Spectrom*, 35 (2000) 337.
7 Sylvia J M, Janni J A, Klein J D & Spencer K M, *Anal Chem*, 72 (2000) 5834.
8 Krausa M & Schorb K, *J Electroanal Chem*, 461 (1999) 10.
9 Junqueira J R C, de Araujo W R, Salles M O & Paixao T R L C, *Talanta*, 104 (2013) 162.
10 Crespy C, Duvauchelle P, Kaftandjian V, Soulez F & Ponard P, *Nucl Instr Methods Phys Res A: Accel Spectrom Detect Assoc Equip*, 623 (2010) 1050.
11 Yinon J & Hwang D-G, *Mass Spectrom Rev*, 1 (1982) 257.
12 Sukhanov P T, Kushnir A A, Churilina E V, Maslova N V & Shatalov G V, *J Anal Chem*, 72 (2017) 468.
13 Germain M E & Knapp M J, *Chem Soc Rev*, 38 (2009) 2543.
14 Sun X, Wang Y & Lei Y, *Chem Soc Rev*, 44 (2015) 8019.
15 Toal S J & Trogler W C, *J Mater Chem*, 16 (2006) 2871.
16 Moore D S, *Rev Sci Instrum*, 75 (2004) 2499.
17 Thomas S W, Joly G D & Swager T M, *Chem Rev*, 107 (2007) 1339.
18 Kobaisi M A, Bhosale S V, Latham K, Raynor A M & Bhosale S V, *Chem Rev*, 116 (2016) 11685.
19 Bhosale S V, Kobaisi M A, Jadhav R W, Morajkar P P, Jones L A & George S, *Chem Soc Rev*, 50 (2021) 9845.
20 Shukla J & Mukhopadhyay P, *Eur J Org Chem*, 2019 (2019) 7770, (https://doi.org/10.1002/ejoc.201901390).
21 Bhosale S V, Bhosale S V & Bhargava S K, *Org Biomol Chem*, 10 (2012) 6455.
22 Perepichka I F & Perepichka D F, *Handbook of Thiophene-based Materials*: *Applications in Organic Electronics and Photonics*, (John Wiley & Sons, Weinheim) 2009.
23 Bhalla V, Gupta A & Kumar M, *Org Lett*, 14 (2012) 3112.
24 Qayyum M, Bushra T, Khan Z A, Gul H, Majeed S, Yu C, Farooq U, Shaikh A J & Shahzad S A, *ACS Omega*, 6 (2021) 25447.
25 Gharib D H, Lock P, Moulton S E & Malherbe F, *ChemNanoMat*, 5 (2019) 1303.
26 Ye Q, Chang J, Huang K-W & Chi C, *Org Lett*, 13 (2011) 5960.
27 Basavaraja J, Inamdar S R & Suresh Kumar H M, *Spectrochim Acta Part A*, 137 (2015) 527.
28 Lakowicz J R, *Principles of Fluorescence Spectroscopy*, 3rd ed., (Springer, New York) 2006.